LETTER

Ultraviolet Photodetector Based on a MgZnO Film Grown by Radio-Frequency Magnetron Sputtering

Yanmin Zhao,[†,‡] Jiying Zhang,[*,†] Dayong Jiang,[†] Chongxin Shan,[†] Zhenzhong Zhang,[†] Bin Yao,[†] Dongxu Zhao,[†] and Dezhen Shen[†]

Key Laboratory of Excited State Processes, Changchun Institute of Optics, Fine Mechanics and Physics, Chinese Academy of Sciences, Changchun 130033, China, and Graduate School of the Chinese Academy of Sciences, Beijing 100049, China

ABSTRACT The metal−semiconductor−metal ultraviolet (UV) photodetector was fabricated on the $Mg_{0.47}Zn_{0.53}O$ layer grown by radio-frequency magnetron cosputtering. The photodetector shows the peak response at 290 nm with a cutoff wavelength at 312 nm. It exhibits a very low dark current of about 3 pA at 5 V bias, and the UV−visible rejection ratio ($R = 290$ nm/$R = 400$ nm) is more than 4 orders of magnitude. The transient response for the detector was measured, and it was found that the rise time is 10 ns and the fall time is 30 ns. The reason for the short response time is related to the Schottky structure.

KEYWORDS: UV photodetector • MSM • $Mg_{0.47}Zn_{0.53}O$ • RF magnetron cosputtering

INTRODUCTION

Ultraviolet (UV) photodetection has drawn a great deal of interest in recent years because of many new requirements brought by various technological developments, such as flame detection, engine monitoring, missile plume detection, chemical sensing, and intersatellite communications (1−5). MgZnO, similar to AlGaN, is an ideal candidate material for UV photodetectors. It possesses tunable band-gap energy (3.3−7.8 eV) (6−8), availability of lattice-matched single-crystal substrates (9), high radiation hardness (10), and low growth temperatures (8). In addition, this material is abundant, inexpensive, and environmentally friendly as well.

Metal−semiconductor−metal (MSM)-structured UV detectors based on $Mg_xZn_{1-x}O$ with both Schottky and Ohmic contacts have been reported (9, 11−18). A photodetector fabricated on $Mg_{0.68}Zn_{0.32}O/SrTiO_3/Si$ shows a peak response at 225 nm, for which the UV−visible rejection ratio is only 1 order of magnitude (13). The detector fabricated on $Mg_{0.34}Zn_{0.66}O$ showed a peak response at 308 nm and a cutoff at 317 nm with a fast rise time of 8 ns, but it has a long fall time with the value of 1.4 μs (11). Our group has reported the UV photodetector on MgZnO films grown by radio-frequency (RF) magnetron sputtering (16, 17), but there are only a few reports on the response time study of the adjacent solar-blind MgZnO UV detector.

In this paper, one MSM photodetector was fabricated on a $Mg_{0.47}Zn_{0.53}O$ thin film grown on a quartz substrate by RF magnetron cosputtering. The results show that a peak photoresponse is at 290 nm and it achieves a fast transient response.

EXPERIMENTAL SECTION

The $Mg_{0.47}Zn_{0.53}O$ thin film was prepared on a quartz substrate by RF magnetron cosputtering from Zn (99.99%) and Mg (99.99%) targets. Each of the targets had a diameter of 3 in. The substrate was cleaned using acetone and ethanol for 5 min in an ultrasonic bath, followed by rinsing with deionized water. The chamber was pumped down to a high vacuum of 10^{-4} Pa by a turbo molecular pump. Then Ar_2 and O_2 gases were introduced into the sputtering chamber through two separate mass-flow controllers with flow rates of 20 and 20 sccm (standard cubic centimeter per minute), respectively. The working pressure in the chamber was kept at 2.0 Pa during film growth. The applied sputtering power to Zn and Mg targets were 100 and 200 W, respectively. The substrate temperature was kept at 600 °C, and the substrate was rotated during deposition to improve the film uniformity.

A Ringaku O/max-RA X-ray diffractometer with Cu Kα radiation ($\lambda = 0.154\,178$ nm) was used to make $\theta-2\theta$ scans to evaluate the crystalline property of $Mg_{0.47}Zn_{0.53}O$. Both optical transmission and absorption spectra were recorded using a Shimadzu UV-3101PC scanning spectrophotometer. A MSM-structured photodetector was fabricated on the $Mg_{0.47}Zn_{0.53}O$ film by depositing interdigital gold electrodes on the film. The current−voltage ($I-V$) curve of the photodetector was measured by a semiconductor parameter analyzer (Keithely 2200). A standard lock-in amplifier was employed for the spectral response measurements, where the irradiation source is a 150 W xenon lamp. The time-resolved response was obtained using a Nd:YAG laser with a wavelength of 266 nm and a pulse width of 10 ns. The transient signal was recorded by a boxcar with 50 Ω impedance.

* E-mail: zhangjy53@yahoo.com.cn. Tel: +86-43186176312. Fax: +86-43186176298.

Received for review August 11, 2009 and accepted October 15, 2009

† Chinese Academy of Sciences.

‡ Graduate School of the Chinese Academy of Sciences.

DOI: 10.1021/am900531u

Published on Web 10/20/2009

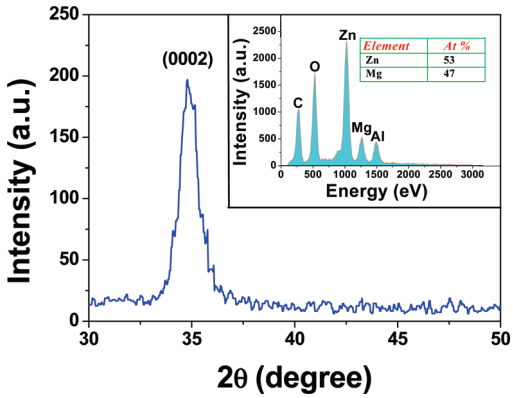

FIGURE 1. XRD spectra of the $Mg_{0.47}Zn_{0.53}O$ thin film grown on quartz prepared by RF magnetron sputtering. The inset is the EDS spectrum of the $Mg_{0.47}Zn_{0.53}O$ film.

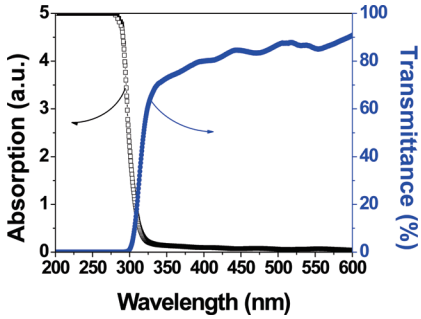

FIGURE 2. UV−visible transmission and absorption spectra of the $Mg_{0.47}Zn_{0.53}O$ film.

RESULTS AND DISCUSSION

Figure 1 shows the X-ray diffraction (XRD) pattern of the MgZnO thin film grown on a quartz substrate. It was noticed that only one diffraction peak is around $2\theta = 34.75°$, which corresponds to the (0002) orientation of the MgZnO hexagonal structure. The absence of characteristic peaks of the cubic phase [such as the (111) peak] indicates that the sample possesses only the wurtzite phase and has the preferred (0002) orientation. The full width at half-maximum (fwhm) value for this sample was 0.5°. The inset shows the energy-dispersive spectrometry (EDS) value of MgZnO, and the Mg/Zn atom ratio is about 0.47/0.53 (the detection limit of EDS is 1%).

Figure 2 shows the transmission and absorption spectra of the $Mg_{0.47}Zn_{0.53}O$ film at room temperature, with the substrate contribution excluded. The transmission spectrum of the film shows more than an 80% transmission ratio in the visible region. The spectrum also has Fabry−Pérot oscillations. There is a steep absorption edge at 307 nm corresponding to an optical band gap of 4.04 eV from the absorption spectrum.

The inset in Figure 3a is the optical micrograph of the $Mg_{0.47}Zn_{0.53}O$-based MSM UV detector. The interdigital metal electrodes, which were defined on a 200 nm gold layer by conventional UV photolithography and a lift-off procedure, are 500 μm long and 5 μm wide and have an interelectrode spacing of 5 μm. In the micrograph, the white and black parts are the electrodes and $Mg_{0.47}Zn_{0.53}O$, respectively. There are 24 fingers in our interdigital structure, 12 up and 12 down.

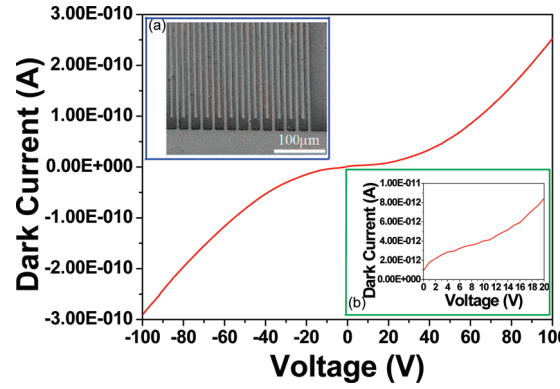

FIGURE 3. $I-V$ characteristics of the $Mg_{0.47}Zn_{0.53}O$-based MSM photodetector. Inset a is the optical microscopic top view of the MSM-structured photodetector showing interdigitated electrodes. Inset b is the $I-V$ characteristics of the $Mg_{0.47}Zn_{0.53}O$-based MSM photodetector on a small voltage scale.

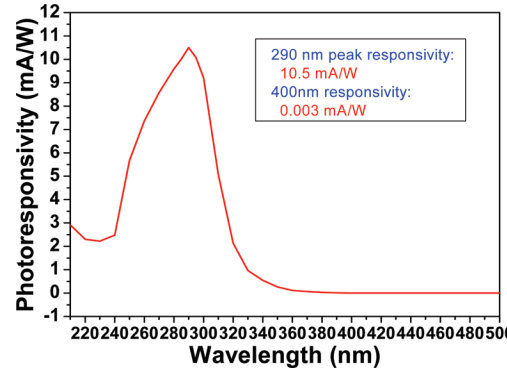

FIGURE 4. Spectral responsivity of the photodetector fabricated from $Mg_{0.47}Zn_{0.53}O$ at a bias of 5 V.

The $I-V$ curve is shown in Figure 3. From the inset in Figure 3b, the device clearly presents a Schottky contact of the MSM structure. At 5 V reverse bias, the dark current is around 3 pA. Furthermore, the value is under 250 pA even up to 100 V bias voltage. The low dark current is helpful for enhancing the detector's signal-to-noise (S/N) ratio because the shot noise, which exceeds the Johnson and $1/f$ noise if the operating frequency is not too low, is proportional to the dark current (13).

The spectral response of the UV detector under front illumination is plotted in Figure 4. The maximum responsivity of the detector is 10.5 mA/W at 290 nm with 5 V bias. The cutoff wavelength is about 312 nm, which is almost in agreement with the absorption edge of $Mg_{0.47}Zn_{0.53}O$ shown in Figure 2. Meanwhile, the UV (290 nm)−visible (400 nm) rejection ratio of the device is more than 4 orders of magnitude, indicating excellent visible blindness. The responsivity of our device is relatively low. The reason for this may be that the crystal quality of this film was not very good (from XRD results in Figure 1), so we suggest that there are many complex defects existing in the film, the result being that some photogenerated carries disappear before reaching the gold poles. In the short UV spectral region, the spectral response of the detector shows a large decrease from 290 to 250 nm. In theory, the penetration depth of light in solid, $d = 1/\alpha$, is defined as the transmitted distance of light when its intensity declines to $1/e$ of the initial value. α is the

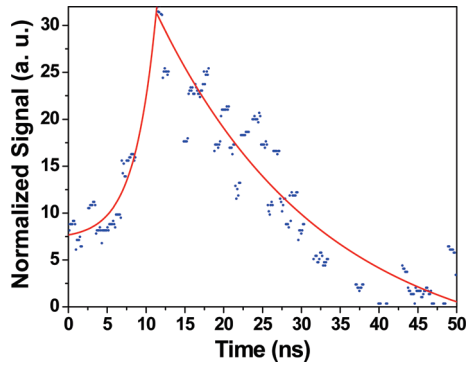

FIGURE 5. Normalized pulse response measurement of the $Mg_{0.47}Zn_{0.53}O$ UV detector excited by Nd:YAG laser pulses (266 nm, ~10 ns).

absorption coefficient. The value α increases as the wavelength becomes shorter, so the reason for the photoresponsivity decrease may be that the penetrating depth of the incident light becomes more shallow as the wavelength becomes shorter, which makes the photogenerated carriers decrease as a result of the decrease in the incident photon number. In contrast, the response of the detector shows an increase from 240 to 210 nm; the reason for this is thought to be that the density of the complex defects in the film surface is less than that of the body, which may be due to the surface recombination caused by etching. The detailed analysis needs further research.

Figure 5 shows the temporal response spectrum of the detector. The detector was connected in series with a load resistor ($R_L = 50\ \Omega$) and biased at 5 V. The photodetector shows a short 10−90% rise time and a 90−10% fall time of 10 and 30 ns, respectively. The valuea are shorter than those published previously (14, 19). The 10 ns rise time is limited by the pulse laser (nominal pulse duration fwhm of 10 ns). In theory, the response time of the photodetector is determined by two main factors: the RC time constant and the time of the carrier across the finger gap. Usually, the response time is significantly dominated by the RC time constant of the device because of the large capacitance for the photovoltaic detector, such as the pn junction and the Schottky contact structures. However, the RC time constant limit could often be neglected for the MSM photodetector because of the small capacitance. In order to count the transit time, another MgZnO thin film with a mobility value of 1.10 $cm^2/V \cdot s$ (20) was selected; at 5 V bias and 5 μm space, the velocity of the electron was 1.1×10^4 cm/s. Under this condition, the estimated value of the transit time from the ratio of the half electrode gap (2.5 μm) to the electron velocity (1.1×10^4 cm/s) is around 22 ns. It is well-known that the expression of the electron mobility is $\mu = 1/nRe$, so the sample used to fabricate the detector in our work has a low mobility value because of the low electron concentration value n and the high resistance value R. In this way, it can be found that the transit time of the detector in our work should be several tens of nanoseconds, which is very close to the response time. Therefore, the transit time limit should be responsible for the transient response. Another factor that affects the temporal response is the excess lifetime of the trapped carriers, especially for the trapped holes in n-type or undopped semiconductors. However, the detector in our work possesses a MSM-structured Schottky property, and the carriers can hardly be trapped. Moreover, the penetration depth of short-wavelength light is shallow, and then photogenerated carriers can be swept out to gold poles quickly. This can be testified from Figure 5, which indicates that no persistent photoconductivity phenomenon is observed.

CONCLUSIONS

In summary, we have demonstrated a MSM-structured UV detector based on a $Mg_{0.47}Zn_{0.53}O$ thin film grown on quartz by RF magnetron cosputtering. The dark current of the detector at 5 V bias is 3 pA. A peak responsivity of 10.5 mA/W located at 290 nm and a cutoff at 312 nm under a 5 V bias were observed. The transient response of the detector showed a fast component with a rise time of 10 ns and a fall time of 30 ns.

Acknowledgment. This work is supported by the Key Project of National Natural Science Foundation of China under Grant 50532050, the 973 program under Grants 2008CB317105 and 2006CB604906, and the Knowledge Innovation Program of the Chinese Academy of Sciences (Grant kjcx3.syw.w01).

REFERENCES AND NOTES

(1) Razeghi, M.; Rogalski, A. *J. Appl. Phys.* **1996**, *79*, 7433–7473.
(2) Liao, M.; Koide, Y. *Appl. Phys. Lett.* **2006**, *89*, 113509 (3pp).
(3) Goldberg, Y. A. *Semicond. Sci. Technol.* **1999**, *14*, R41–R60.
(4) Ohta, H.; Hosono, H. *Mater. Today* **2004**, *7*, 42–51.
(5) Moon, T. H.; Jeong, M. C.; Lee, W.; Myoung, J. M. *Appl. Surf. Sci.* **2005**, *240*, 280–285.
(6) Narayan, J.; Sharma, A. K.; Kvit, A.; Jin, C.; Muth, J. F.; Holland, O. W. *Solid State Commun.* **2002**, *121*, 9–13.
(7) Ohtomo, A.; Kawasaki, M.; Koida, T.; Masubuchi, K.; Koinuma, H.; Sakurai, Y.; Yoshida, Y.; Yasuda, T.; Segawa, Y. *Appl. Phys. Lett.* **1998**, *72*, 2466–2468.
(8) Choopun, S.; Vispute, R. D.; Yang, W.; Sharma, R. P.; Venkatesan, T.; Shen, H. *Appl. Phys. Lett.* **2002**, *80*, 1529–1531.
(9) Hullavarad, S. S.; Dhar, S.; Varughese, B.; Takeuchi, I.; Venkatesan, T.; Vispute, R. D. *J. Vac. Sci. Technol. A* **2005**, *23*, 982–985.
(10) Auret, F. D.; Goodman, S. A.; Hayes, M.; Legodi, M. J.; van Laarhoven, H. A.; Look, D. C. *Appl. Phys. Lett.* **2001**, *79*, 3074–3076.
(11) Yang, W.; Vispute, R. D.; Choopun, S.; Sharma, R. P.; Venkatesan, T.; Shen, H. *Appl. Phys. Lett.* **2001**, *78*, 2787–2789.
(12) Koike, K.; Hama, K.; Nakashima, I.; Takada, G.; Ogata, K.; Sasa, S.; Inoue, M.; Yano, M. *J. Cryst. Growth* **2005**, *278*, 288–292.
(13) Yang, W.; Hullavarad, S. S.; Nagaraj, B.; Takeuchi, I.; Sharma, R. P.; Venkatesan, T.; Vispute, R. D.; Shen, H. *Appl. Phys. Lett.* **2001**, *82*, 3424–3426.
(14) Liu, K. W.; Zhang, J. Y.; Ma, J. G.; Jiang, D. Y.; Lu, Y. M.; Yao, B.; Li, B. H.; Zhao, D. X.; Zhang, Z. Z.; Shen, D. Z. *J. Phys. D: Appl. Phys.* **2007**, *40*, 2765–2768.
(15) Jiang, D. Y.; Shan, C. X.; Zhang, J. Y.; Lu, Y. M.; Yao, B.; Zhao, D. X.; Zhang, Z. Z.; Shen, D. Z.; Yang, C. L. *J. Phys. D: Appl. Phys.* **2009**, *42*, 025106 (3pp).
(16) Jiang, D. Y.; Shan, C. X.; Zhang, J. Y.; Lu, Y. M.; Yao, B.; Zhao, D. X.; Zhang, Z. Z.; Fan, X. W.; Shen, D. Z. *J. Cryst. Growth Des.* **2009**, *9*, 454–456.
(17) Liu, K. W.; Shen, D. Z.; Shan, C. X.; Zhang, J. Y.; Jiang, D. Y.; Zhao, Y. M.; Yao, B.; Zhao, D. X. *J. Phys. D: Appl. Phys.* **2008**, *41*, 125104 (3pp).
(18) Jiang, D. Y.; Zhang, J. Y.; Liu, K. W.; Zhao, Y. M.; Cong, C. X.; Lu, Y. M.; Yao, B.; Zhang, Z. Z.; Shen, D. Z. *Semicond. Sci. Technol.* **2007**, *22*, 687–690.
(19) Jiang, D. Y.; Zhang, J. Y.; Lu, Y. M.; Liu, K. W.; Zhao, D. X.; Zhang, Z. Z.; Shen, D. Z.; Fan, X. W. *Solid-State Electron.* **2008**, *52*, 679–682.
(20) Wei, Z. P.; Yao, B.; Zhang, Z. Z.; Lu, Y. M.; Shen, D. Z.; Li, B. H.; Wang, X. H.; Zhang, J. Y.; Zhao, D. X.; Fan, X. W.; Tang, Z. K. *Appl. Phys. Lett.* **2006**, *89*, 102104 (3pp).

AM900531U